

Structure functions of rod-like DNA fragment and polystyrenesulfonate solutions in the modified Poisson–Boltzmann theory[☆]

L.B. Bhuiyan^{a,*}, C.W. Outhwaite^b, J.R.C. van der Maarel^c

^a *Laboratory of Theoretical Physics, Department of Physics, Box 23343, University of Puerto Rico, Rio Piedras, Puerto Rico 00931-3343, USA*

^b *School of Mathematics, University of Sheffield, Sheffield S3 7RH, UK*

^c *Department of Physical and Macromolecular Chemistry, Gorlaeus Laboratories, Leiden University, 2300 RA Leiden, The Netherlands*

Abstract

The partial structure functions of aqueous solutions of rod-like DNA fragments and polystyrenesulfonic acid are calculated in the modified Poisson–Boltzmann theory. The cylindrical cell model appropriate for linear polyelectrolyte solutions with monovalent counterions and without any added salt is utilized. The predicted results are compared with the corresponding results from the classical Poisson–Boltzmann theory, and experimental small angle neutron scattering data obtained in the monomer concentration range 0.05–0.2 mol/dm³. It is seen that both the modified Poisson–Boltzmann and the Poisson–Boltzmann results lead to a very good fit to the experimental structure functions.

1. Introduction

A widely used model in the theoretical studies and interpretation of many of the experimental thermodynamic data of linear polyelectrolyte solutions is the cylindrical cell model [1]. In the traditional approach, the cell model is used in conjunction with the classical Poisson–Boltzmann (PB) theory, and the availability of exact analytical solution to the PB equation when a single species counterion is present in the cell [2, 3] has lead to numerous applications of the equation (see for example, reviews [1, 4]). In this model the polyion is treated as a symmetrically charged rigid cylinder, or line, and end effects are neglected in most cases so that cylindrical symmetry applies. The

[☆] It is a pleasure to dedicate this paper to Dr. S.H. Chen on the occasion of his sixtieth birthday.

* Corresponding author.

polyion is then placed along the axis of a cell of same geometry, the polyion being surrounded by a proportionate number of mobile simple ions such that the cell is electrically neutral. There is a practical relevance for polyelectrolyte–simple electrolyte systems in that many real systems of biological significance (e.g., DNA, proteins) and industrial significance (e.g., detergents, cosmetics, gels) belong to this class.

Over the last decade formal statistical mechanical methods used in the planar electric double layer research have been adapted to describe the cylindrical ionic atmosphere. For example, the cylindrical cell model has been treated in the hypernetted chain/mean spherical approximation (HNC/MSA) [5], a truncated modified Poisson–Boltzmann (MPB) theory [6], and the full MPB theory [7]. Simultaneous Monte-Carlo (MC) simulations have also been performed [6–8]. The recent MPB work [7] in particular, shows the theoretical predictions to be in very good agreement overall with the MC results for both mono- and divalent ion systems. The classical PB theory on the other hand, while adequate for monovalent systems at low concentrations, tends to deviate from the simulations as the concentration is raised when the ionic correlation and exclusion volume effects, neglected in the mean field approximation, become important. The MPB formulation seeks to account for these effects in a potential approach, and has been one of the most successful theories in describing the electric double layer phenomena in planar, spherical, and cylindrical geometries [9–11].

Parrallel to these theoretical developments, accurate small angle neutron scattering data on systems such as solutions of DNA fragments [12, 13], polystyrenesulfonates (PSS) [14], and micelles [15] have also begun to be available in recent years. Techniques based on the variation of isotopic composition of solvent, often called the solvent contrast method [16], have enabled partial structure functions in these systems to be determined and thus a complete picture of the structure obtained. For the rod-like DNA fragments and PSS solutions without any added salt, it was seen that by optimizing some of the geometric parameters of the relevant cell models, the PB theory can give a good fit to the partial structure functions in the experimental concentration range of 0.05–0.2 mol/dm³. Motivated by the success of the MPB theory in reproducing the MC data for the cylindrical cell models [7], we thought it of interest to compare the predictions of the theory with the experimental scattering results for DNA and PSS solutions.

It ought to be mentioned here that by its nature the cell model excludes intercellular correlations. Indeed there is evidence [7] that at higher concentrations, and particularly so when divalent ions are present, these correlations may become substantial so that the concept of an isolated cell might be in question. However, for the monovalent counterion systems in the concentration range considered in the present work, the model would be expected to be reliable.

2. Theory

The geometric parameters involved in the cylindrical cell model, the Hamiltonian, and the MPB formulation of the model have been discussed previously in some detail in

Ref. [7]. We shall therefore confine ourselves here to outlining the principal equations following the notations used in [7].

We assume the fully extended, linear rod-like polymer (polyion) of length h and radius R_p to consist of N monomer units of length b each so that $h = Nb$. The polyion is placed along the axis of a cylinder of same length and radius R_c , and carries a total charge $-Ne_0$ (e_0 is the proton charge) distributed uniformly. The cell radius R_c is related to the monomer number density n_m through

$$n_m = 1/(\pi R_c^2 b). \quad (1)$$

The polyion is bathed by a single species neutralizing mobile simple ions of common diameter a and having a distance of closest approach $a_p (= R_p + a/2)$ to the polyion. Allowing the centres of the simple ions to go upto R_c , in the MPB analysis the distribution of the counterions (at a perpendicular distance r from the axis) with respect to the polyion is given by

$$g(r) = \left(\frac{\xi(r)}{\xi(R_c)} \right) g(R_c) \exp \left[-\frac{\beta Z^2 e_0^2}{2\epsilon a} (F - F_c) - \beta Z e_0 \{L[u(r)] - L[u(R_c)]\} \right], \quad (2)$$

where $u(r) = \sqrt{r}\psi(r)$, $\psi(r)$ being the mean electrostatic potential. Z is the valency of the counterions, ϵ is the permittivity of the solution, and $\beta = 1/(k_B T)$. The quantities $L[u]$, F , and F_c are given by

$$L[u] = \frac{F}{2\sqrt{r}} [u(r+a) + u(r-a)] - \frac{F-1}{2a\sqrt{r}} \int_{r-a}^{r+a} u(R) dR, \quad (3)$$

$$F = \begin{cases} 1/\{(1+\kappa a) - (\kappa a/\pi)S\}, & a_p \leq r \leq R_p + 3a/2, \\ 1/(1+\kappa a), & r \geq R_p + 3a/2, \end{cases} \quad (4)$$

$$F_c = F(R_c), \quad (5)$$

$$S = \int_{\theta_0}^{\pi/2} \sin \theta \cos^{-1} \left\{ \frac{c - \cos^2 \theta}{(2r/a) \sin \theta} \right\} d\theta,$$

$$\theta_0 = \sin^{-1} \left[\frac{r - a_p}{a} \right], \quad c = 1 - \left(\frac{a_p}{a} \right)^2 + \left(\frac{r}{a} \right)^2, \quad (6)$$

where κ is the local Debye–Hückel parameter

$$\kappa^2 = \frac{4\pi\beta e_0^2}{\epsilon} Z^2 n(r), \quad n(r) = ng(r) \quad (7)$$

and n is the average number density of the counterions.

The exclusion volume term $\xi(r)$ is evaluated from the Bogoliubov–Born–Green–Yvon hierarchy and is

$$\begin{aligned}\xi(r) &= g(r|Z=0) \\ &= H(r-a_p) \exp \left[2\pi \int_r^{R_c} n \int_{\max(a_p, y-a)}^{\min(R_c, y+a)} (X-y)g(X) \right. \\ &\quad \left. \times \exp \{-\beta Ze_0 \phi(y, X)\} dX dy \right],\end{aligned}\quad (8)$$

$$\phi(y, X) = \frac{F}{4\pi a} \int_{V_d} \nabla^2 \psi dV. \quad (9)$$

$H(x)$ is the Heaviside function and $\phi(y, x)$ is the fluctuation potential calculated on the exclusion surface of the discharged ion of volume V_d .

The mean electrostatic potential $\psi(r)$ and $g(r)$ satisfy the Poisson equation

$$\frac{1}{r} \frac{d\psi(r)}{dr} \left(r \frac{d\psi(r)}{dr} \right) = -\frac{4\pi e_0}{\varepsilon} Zng(r) \quad (10)$$

subject to the boundary conditions

$$\left. \frac{d\psi(r)}{dr} \right|_{r=R_c} = 0 \quad (11)$$

and

$$\left. \frac{d\psi(r)}{dr} \right|_{r=a_p} = -2Ne_0/(\varepsilon ha_p). \quad (12)$$

The classical PB theory is recovered upon setting $\xi(r) = 1$, $F = F_c$, and taking the limit $a \rightarrow 0$ in Eq. (3).

The partial structure functions for the cylindrically symmetric geometry, and neglecting intercellular correlations have been derived by van der Maarel et al [12]. These read

$$S_{ij} = \frac{1}{N} \int_0^1 \left[\frac{\sin(q\mu h/2)}{(q\mu h/2)} \right]^2 P_i(q, \mu) P_j(q, \mu) d\mu, \quad (13)$$

$$P_i = 2\pi h \int_0^{R_c} r J_0 \left(qr \sqrt{1-\mu^2} \right) n_i(r) dr. \quad (14)$$

Here, the subscripts i, j refer to the monomer (m) or to the counterion (c), q is the magnitude of the momentum transfer vector \mathbf{q} , and $J_0(x)$ is the zeroeth order Bessel

function. We note that the monomer distribution is usually assumed to be a step function so that

$$P_m(q, \mu) = 2N \frac{J_1 \left(qR_p \sqrt{(1 - \mu^2)} \right)}{\left(qR_p \sqrt{(1 - \mu^2)} \right)}, \quad (15)$$

$J_1(x)$ being the first-order Bessel function.

3. Results and discussion

The experimental partial structure functions for 163 base-pairs DNA and PSS solutions were obtained by small angle neutron scattering and contrast matching in water [12–14]. In both cases the counterion was tetramethylammonium (TMA) and there was no excess simple salt in solution. The structure functions are displayed in Figs. 1 and 2 for 0.05 mol nucleotides/dm³ DNA and 0.1 mol/dm³ PSS respectively. More data on 0.1 mol nucleotide/dm³ DNA and 0.2 mol/dm³ PSS are available. However, these supplementary data show similar qualitative and quantitative features and are not presented here. All data were obtained using small angle scattering instruments D17 and PACE, situated on the nuclear reactor cold sources at the Institute Laue-Langevin, Grenoble, and Laboratoire Léon Brillouin, Saclay, respectively.

The DNA fragments can be considered rod-like, since the contour length (55 nm) is approximately equal to the persistence length (40 nm). Accordingly, the monomer–monomer partial structure function, S_{mm} , can be compared to the form function of a uniform rod, provided that the intermolecular interferences are negligible. This condition is satisfied for sufficiently high values of momentum transfer or by performing experiments at low concentrations. With present day technology, the lower DNA concentration limit is set at 0.05 mol nucleotides/dm³. As can be seen in Fig. 1 (top), for $q < 1 \text{ nm}^{-1}$ intermolecular interferences become progressively more important and the DNA monomer–monomer structure function deviates from the form function. In the high q region, the form function was optimized to the data by variation of the monomer unit length b and radius R_p . These parameters take the values 0.171 nm and 0.8 nm, respectively, in close agreement with the expected values for a double helix in the B-form. The fragment length was taken to be 50 nm, and it was checked that in the present range of momentum transfer there is no significant influence of DNA flexibility.

For PSS the situation is more complicated due to the high intrinsic polyion flexibility (short persistence length). Here, the polyion is modelled as a sequence of rod-like segments with a length equal to the Kuhn length, being twice the persistence length. For sufficiently high values of momentum transfer the local structure is probed and interferences between different chain segments (both intra- and intermolecular) can be neglected. As can be seen in Fig. 2 (top), in the q range 0.75–1.3 nm^{−1} the deviation of the rigid segment form function from the experimental data is more pronounced than in

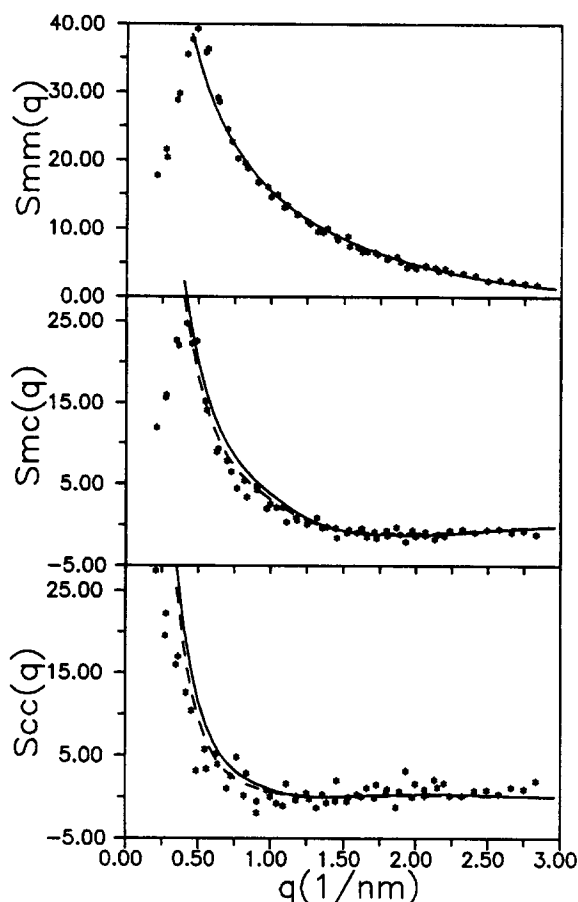


Fig. 1. The partial structure functions for 0.05 mol nucleotides/dm³ DNA. From top to bottom: monomer–monomer, S_{mm} ; monomer–counterion, S_{mc} ; counterion–counterion, S_{cc} . The stars are the experimental neutron scattering results, the solid lines represent the modified Poisson–Boltzmann results, whereas the dashed lines are calculated with the Poisson–Boltzmann theory. In case of the monomer–monomer structure, the solid line denotes the form function of a uniform segment.

the case of DNA. This is due to the short persistence length and enhanced flexibility. The derived values of the monomer unit length b and radius R_p are 0.164 nm and 0.6 nm, respectively. The segment length was chosen to be 15 nm, but the actual value has only a minor effect on the derived values of b and R_p . The radius R_p agrees reasonably with the backbone structure, but b is significantly smaller than the value expected for the fully stretched (all trans) configuration.

The theoretical monomer–counterion and counterion–counterion partial structure functions were calculated using the transformation Eqs. (13) and (14), together with the radial counterion distribution function. The radial distribution function was obtained from either the classical PB or the MPB theory in the cell model. The parameters

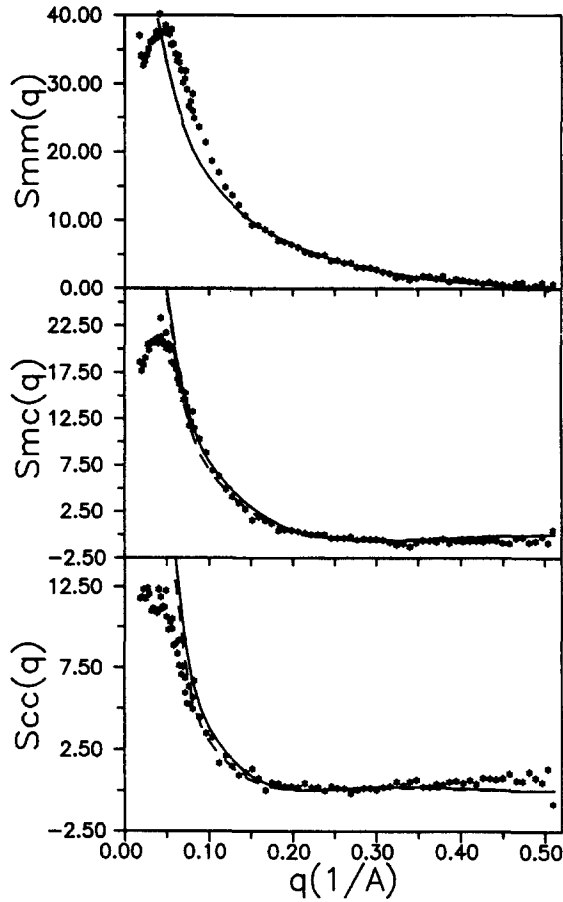


Fig. 2. As in Fig. 1, but for 0.1 mole/dm³ PSS.

b and R_p were fixed at the values obtained from the polymer structure, whereas the cell radius is given by concentration (Eq. (1)). The distance of closest approach was obtained by optimizing the PB results to the experimental data. This parameter takes the values $a_p = 1.4$ nm and 0.9 nm, for DNA and PSS, respectively. These values are in agreement with the sum of the polyion outer radius and the TMA radius (including hydration effects). The temperature was fixed at that for the experiments, i.e., 293 K, with a Bjerrum length 0.71 nm appropriate for water. The dashed lines in Figs. 1 and 2 refer to the classical PB results, whereas the solid lines are calculated with the MPB theory (with the same parameters!).

It is seen in Figs. 1 and 2 that there is excellent agreement between the classical and the modified Poisson–Boltzmann results for both the monomer–counterion (middle) and counterion–counterion (bottom) partial structure functions. This is not surprising, because it is known that for monovalent simple ions and low concentrations

such as the present range, both approaches yield similar radial counterion profiles [7]. This is of course consistent with the comparative behaviour of the PB and formal theories in the electric double layer phenomena [9–11]. At higher concentrations, however, the interionic correlations and ionic exclusion volume effects become important leading to deviations between the classical mean field and, for example, the MPB theories. The same would be true, at a more pronounced scale, for divalent counterion systems [7].

For sufficiently high values of $q (> 1 \text{ nm}^{-1})$ interference effects between different cell volumes are immaterial and the current cell model calculations are in very good agreement with the experimental data. To describe the data in the low q region a complete analysis of the pair correlations of two highly charged polyions (or segments thereof) and their double layers is necessary. The fact that the PB results are a little closer to the experimental data in some regions of the plots is due to the optimization procedure for the distance of closest approach a_p . A small change in a_p would bring the MPB theory in equally good or better agreement.

4. Conclusion

The DNA molecule is suitable for a critical test of the theoretical results. It has a rather rigid molecular structure and the molecular dimensions are fairly well known. There is little doubt about its linear charge density and the colligative properties are in excellent agreement with the predictions based on the cell model [1]. For wave vectors corresponding to the inverse double layer thickness the DNA flexibility can be neglected. The structural parameters derived from the neutron scattering experiments [12–13] are in agreement with the expected dimensions of a double helix in the B-form. Using these molecular parameters, the counterion profile in the radial direction away from the DNA axis can be calculated either on the basis of the classical PB theory or the MPB theory. The partial structure functions were calculated by Fourier transformation of the counterion profile. For monovalent counterions, and in the present concentration range, there are few differences between the theoretical predictions. There is also a nice agreement with both the monomer-counterion and the counterion-counterion experimental partial structure functions, provided that interference effects between different cell volumes are negligible.

For the more flexible PSS polyion similar conclusions can be reached. However, the derived linear charge density, expected on the basis of the fully stretched molecular configuration, is similar to or higher than that in DNA. This was also indicated by the value of the osmotic coefficient for vinylic polyelectrolytes [4]. The partial structure functions for PSS (Fig. 2) are similar to those obtained for DNA (Fig. 1). This immediately confirms the similarity of the local rod-like structure of both polyions.

Acknowledgements

This work was partially supported by the National Science Foundation through Grant CHE-9417824. LBB acknowledges an internal grant through FIPI, University of Puerto Rico.

References

- [1] A. Katchalsky, *Pure Appl. Chem.* 26 (1971) 327.
- [2] R.M. Fuoss, A. Katchalsky and S. Lifson, *Proc. Natl. Acad. Sci. U.S.A.* 37 (1951) 579.
- [3] T. Alfrey Jr., P.W. Berg and H. Morawetz, *J. Polym. Sci.* 7 (1951) 543.
- [4] D. Dolar, in: *Polyelectrolytes*, eds. E. Sélégny, M. Mandel and U.P. Strauss (Reidel, Dordrecht, 1972), p. 97.
- [5] V. Vlachy and D.A. McQuarrie, *J. Chem. Phys.* 83 (1985) 1927.
- [6] D. Bratko and V. Vlachy, *Chem. Phys. Lett.* 90 (1982) 434; 115 (1985) 294.
- [7] T. Das, D. Bratko, L.B. Bhuiyan and C.W. Outhwaite, *J. Phys. Chem.* 99 (1995) 410.
- [8] M. Le Bret and B.H. Zimm, *Biopolymers* 23 (1984) 271; V. Vlachy and A.D.J. Haymet, *J. Chem. Phys.* 84 (1986) 5874; P. Mills, C.F. Anderson and M.T. Record Jr., *J. Phys. Chem.* 89 (1985) 3984.
- [9] S.L. Carnie and G.M. Torrie, *Adv. Chem. Phys.* 56 (1984) 141.
- [10] C.W. Outhwaite and L.B. Bhuiyan, *Mol. Phys.* 74 (1991) 367.
- [11] L.B. Bhuiyan and C.W. Outhwaite, in: *Condensed Matter Theories*, eds. L. Blum and F.B. Malik (Plenum, New York, 1993) Vol. 8, p. 551.
- [12] J.R.C. van der Maarel, L.C.A. Groot, M. Mandel, W. Jesse, G. Jannink and V. Rodriguez, *J. Phys. II France* 2 (1992) 109.
- [13] L.C.A. Groot, M.E. Kuil, J.C. Leyte, J.R.C. van der Maarel, J.P. Cotton and G. Jannink, *J. Phys. Chem.* 98 (1994) 10167.
- [14] J.R.C. van der Maarel, L.C.A. Groot, J.G. Hollander, W. Jesse, M.E. Kuil, J.C. Leyte, L.H. Leyte-Zuiderweg, M. Mandel, J.P. Cotton, G. Jannink, A. Lapp and B. Farago, *Macromolecules* 26 (1993) 7295.
- [15] P.J. Derian, L. Belloni and M. Drifford, *Europhys. Lett.* 7 (1988) 243.
- [16] B. Jacrot, *Rep. Prog. Phys.* 39 (1976) 911.